Electrogenerated Chemiluminescence of a Series of Donor−Acceptor Molecules and X-ray Crystallographic Evidence for the Reaction Mechanisms

Xiao Jiang,[†] Xichuan Yang,*[,†] Changzhi Zhao,[‡] Kun Jin,[†] and Licheng Sun*[,†,§]

State Key Laboratory of Fine Chemicals, DUT-KTH Joint Education and Research Center on Molecular Devices, Dalian University of Technology (DUT), 158 Zhongshan Road, 116012 Dalian, China, College of Chemistry and Molecular Engineering, Qingdao University of Science and Technology, 53 Zhengzhou Road, 266042 Qingdao, China, and KTH School of Chemical Science and Engineering, Organic Chemistry, Teknikringen 30, 10044 Stockholm, Sweden

Received: February 5, 2007; In Final Form: April 26, 2007

Three series of donor−acceptor π-conjugated (D-π-A) molecules **1**−**3** have been synthesized with a 2,3,6,7-tetrahydro-1*H*,5*H*-pyrido[3,2,1-*ij*]quinolinyl (Julolidine group), *N*,*N*-dimethylamino, or *N*,*N*-diphenylamino group as the donor moiety, a phenylvinyl or thienylvinyl unit as the bridge, and a bromide or aldehyde group as the acceptor moiety. The photophysical, electrochemical, and electrogenerated chemiluminescence (ECL) characters of these compounds have been studied in a 1:1 PhH/MeCN solution. Three different categories of ECL mechanisms for each of the three families of compounds are discussed, respectively. Compounds **1a**−**c** produce typical and simple monomer ECL emission resulting from the annihilation of their radical cations and radical anions. The ECL emission of compounds **2a**−**c** can be ascribed as an excimer emission. Compounds **3a**−**c** exhibit an aggregate ECL emission. X-ray crystal structures of compounds **1b**, **2a**, and **3a** provide further proof for the above-mentioned reaction mechanisms. All these compounds show stable ECL emission via the singlet excited state without the addition of any co-reactant or additional compound.

Introduction

Electrogenerated chemiluminescence (ECL) is a means of converting electrical energy into radiative energy. It is the luminescence generated by relaxation of excited-state molecules that are produced directly or indirectly by electrochemical reactions. ECL has become an important and valuable detection method in analytical chemistry in recent years.[1] By employing ECL-active species as labels on biological molecules, this method has found wide application in immunoassays and DNA analyses.[2] Commercial systems have been developed that use ECL to detect many clinically important analytes with very high sensitivity and selectivity.[2] Furthermore, it is also an excellent model for investigating the mechanism of electron transfer.[3] The excited state formed in an ECL reaction is similar to that formed during photoexcited fluorescence. However, ECL is considered superior to fluorescence techniques in certain analytical studies because it does not require an external light source for excitation, which may cause signal disturbance in the measurements.[1a]

In 1927, Dufford reported the light emission of Grignard compounds at applied potentials.[4] Up to the present, many studies that focused on the mechanism and nature of ECL have been performed upon polyaromatic hydrocarbons (PAHs) and metal complexes.[5,6] Among them, the most attention has been paid to the ECL reaction based on the ruthenium polypyridine complexes, especially $Ru(bpy)_3^{2+}$ and its derivatives. This is due to their high sensitivity, high stability, and capability of undergoing ECL under moderate conditions in aqueous buffered solutions. More importantly, they have shown extensive practical applications.[7,8]

Recently, organic compounds capable of generating ECL have also attracted attention.[3,9−11] Useful ECL compounds must be able to generate stable radical cations and anions with sufficient energy in the electron-transfer reaction to generate an excited state that emits light with high quantum efficiency. In some cases, however, an additional compound or a co-reactant must be added to assist in the generation of a stable radical counterion which is required for annihilation. These are known as mixed systems and are fairly common among organic ECL systems.[12] Our interests are in those molecules which have simple structures, are facile in their application, and are efficient in generating ECL without the addition of any co-reactant or additional compound.

The donor−acceptor π-conjugated (D-π-A) systems have in recent years been the subject of renewed interest, due to their potential applications in modern photoelectronic technology such as light-emitting diodes and field-effect transistors.[10e] Several donor−acceptor molecules which are mostly linked by a conjugated double or triple bond such as 10-methylphenolthiazine derivatives,[3] phenylquinolinylethyne derivatives,[11a] arylethynylacridine derivatives,[11b] and related compounds, [10c−e,14a] have been reported to have ECL properties.

In this paper, we describe the synthesis of three series of ethylene-based donor−acceptor molecules **1**−**3**, their photophysical, electrochemical, and ECL behavior, and the possible mechanisms for the ECL formation with the assistance of X-ray crystallographic data. The structures of molecules **1**−**3** are shown in Chart 1.

Experimental Section

Materials. *n*-BuLi 2.57 M in hexane, tetra-*n*-butylammonium hexafluorophosphate ($TBAPF_6$), and anhydrous acetonitrile (chromatographic grade) were obtained from Aldrich and used

* Corresponding authors. E-mail: yangxc@dlut.edu.cn (Yang); lichengs@kth.se (Sun).
[†] Dalian University of Technology.
[‡] Qingdao University of Science and Technology.
[§] KTH School of Chemical Science and Engineering, Organic Chemistry.

10.1021/jp071015n CCC: $37.00
Published on Web 06/05/2007

CHART 1: Structures of D-π-A Molecules of Series 1−3

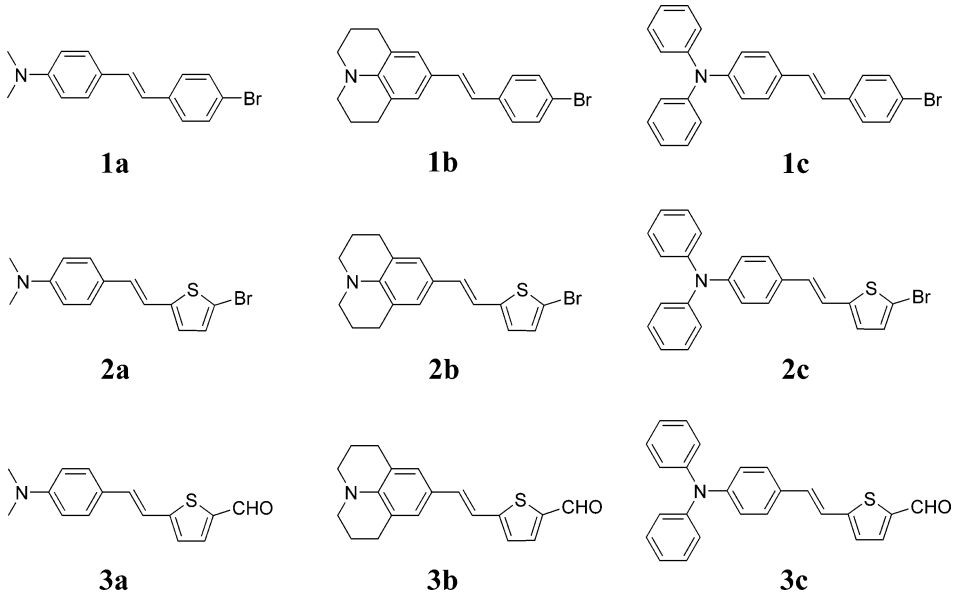

as received. 4-Diphenylamino-benzaldehyde, 2,3,6,7-tetrahydro-1*H*,5*H*-pyrido[3,2,1-*ij*]quinoline-9-carbaldehyde, and diethyl [(5-bromothien-2-yl)methyl]phosphonate were prepared in house. Solvents were distilled according to the standard methods and purged with nitrogen before use. Tetrahydrofuran (THF) and benzene were purified by distillation over sodium chips and benzophenone under a N_2 atmosphere. *N*,*N*-Dimethylformamide (DMF) was dried over 4 Å molecular sieves and purified further by vacuum distillation over calcined baryta. All other solvents and reagents were of analytical grade quality purchased commercially and used as received unless otherwise stated.

Characterization. ^{1}H NMR spectra were recorded on a VARIAN INOVA 400 MHz NMR instrument, and ^{13}C NMR spectra were recorded on the same instrument at 100 MHz. HRMS spectra were recorded with a GC-TOF mass spectrometer (Micromass). All the melting points were not corrected.

All UV−vis spectra were measured on a HP-8453 spectrophotometer in a 1:1 PhH/MeCN mixed solvent by using either a normal sample cell (1 cm), when the solution concentration is below 1×10^{-4} M, or two pieces of glass (1 mm in thickness and 1 cm in width) instead of a normal sample cell with one drop of sample solution penetrating inside them via capillary action, when the solution concentration exceeded 1×10^{-3} M. All fluorescence spectra were recorded on a PTI-C-700 Felix fluorescence spectrophotometer. Fluorescence quantum yields (Φ) were determined in CH_3CN with reference to quinine sulfate ($\Phi = 0.508$ in 0.05 M H_2SO_4).[13]

Cyclic voltammograms were performed with a BAS-100W Electrochemical Work Station using a three-electrode conventional electrochemical cell. Measurements were obtained with 10^{-3} M solution of the compounds in 1:1 PhH/ MeCN mixed solvent with 0.05 M $TBAPF_6$. A platinum disk was used as the working electrode, a platinum wire served as a counter electrode, a Ag/Ag^+ electrode was utilized as a reference electrode, and the scan rate was 100 mV s^{-1}. All potentials were calibrated versus an aqueous SCE by the addition of ferrocene as an internal standard taking $E°$ (Fc/Fc^+) = 0.424 V vs SCE.[3a,15]

ECL spectra were recorded at room temperature using a setup consisting of a fluorescence spectrophotometer and a cyclic voltammograph with a computer interface.[16] Measurements were obtained with 10^{-3} M solution of the compounds in 1:1 PhH/ MeCN mixed solvent with 0.05 M $TBAPF_6$. To generate the annihilation reaction, the platinum electrode was pulsed between the first reduction and first oxidation potentials with a pulse width of 0.5 s.

Crystal X-ray diffraction data of compounds **1b**, **2a**, and **3a** were collected at 273 K with a Siemens SMART CCD diffractometer using graphite monochromated Mo Kα radiation ($\lambda = 0.71073$ Å). The structures were solved by direct methods and subsequent difference Fourier syntheses, and they were refined by the full-matrix least-squares (F^2) on using the SHELXL-97 program. The hydrogen atoms were placed in calculated positions and were held riding on their parent non-hydrogen atoms during the subsequent refinement calculations. All non-hydrogen atoms were refined with anisotropic thermal displacement parameters.

Results and Discussion

Synthesis and Characterization. The structures of D-π-A molecules **1**−**3** are shown in Chart 1. All these compounds have been prepared according to a general synthetic methodology. Series **1** compounds were obtained according to the literature method.[17] The starting material of 4-bromobenzylbromide reacts with triethylphosphite to yield the intermediate of (4-bromobenzyl)phosphonic acid diethyl ester. The intermediate is allowed to react directly without purification with the corresponding aldehyde in the presence of NaH via Horner-Emmons Witting condition, leading to compounds **1a**−**c**. The other intermediate of diethyl[(5-bromothien-2-yl)methyl]phosphonate obtained with 2-bromothiophene as the starting material was also directly used for the preparation of series **2** compounds without further purification. The compounds in series **2** were prepared by a procedure similar to those in series **1**. It should be noted that compound **2b** was difficult to purify because of its great viscidity and poor solubility, so it was used through rough purification in the next synthesis step. Series **2** compounds were formylated in the presence of *n*-BuLi by the Vilsmeier reaction to give series **3** compounds. Most of the molecular structures were characterized by ^{1}H NMR, ^{13}C NMR, and HRMS. The ^{1}H NMR analyses of each compound show that the carbon−carbon double bond connecting the electron donor and acceptor is in *E* configuration as confirmed by a coupling constant $J \geq 16.0$ Hz. Details on the synthesis and NMR characterization are presented in the Supporting Information.

TABLE 1: Photophysical Data of Series 1−3 in 1:1 PhH/MeCN

compound	λ_{abs} (nm)	E_g[a] (eV)	ϵ_{max}[b]	λ_{em} (nm)	$\Delta\lambda_{st}$[c] (nm)	Φ[d]
1a	364	2.97	4.41	452	88	0.229
1b	382	2.79	4.16	479	97	0.075
1c	374	2.90	4.02	464	90	0.175
2a	376	2.84	2.95	460	84	0.135
2c	382	2.81	2.15	473	91	0.095
3a	426	2.32	2.88	600	174	0.279
3b	462	2.19	3.09	633	171	0.233
3c	428	2.43	2.27	594	166	0.264

[a] Calculated from λ_{onset} in absorption spectrum. [b] ($\times 10^4$ M^{-1} cm^{-1}). [c] $\Delta\lambda_{st} = \lambda_{em} - \lambda_{abs}$. [d] Fluorescence quantum yields (Φ) were measured in MeCN with reference to quinine sulfate (Φ = 0.508 in 0.05 M H_2SO_4).[13]

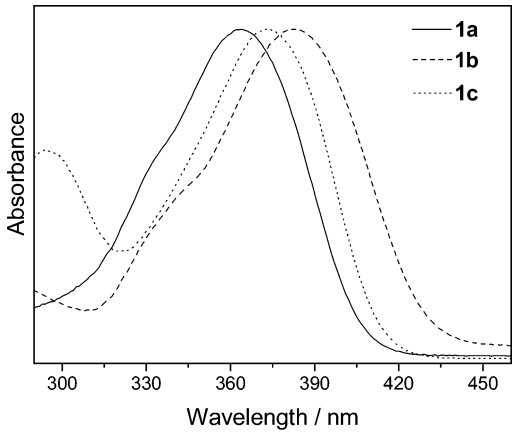

Figure 1. Absorption spectra of **1a** (solid, left), **1b** (dash, right), and **1c** (dot, middle) in 1:1 PhH/MeCN.

Absorption and Emission Spectroscopy. The absorption and emission data of series **1**−**3** in a 1:1 PhH/MeCN solution at a concentration of 1×10^{-5} M are listed in Table 1. In series **1** compounds (**1a**, **1b**, **1c**, Figure 1) the bridge units and electron-withdrawing substituents are the same, but the electron-donor parts are different. Compared with compounds **1a** and **1c**, the rigid ring structure at the end of the electron-donor group in **1b** avoids free rotation of the N−C bond and thus the electron-donating ability of the substituent is enhanced.[14a] Compound **1c** bearing the *N*,*N*-diphenylamino group shows better conjugation effect than **1a** bearing the *N*,*N*-dimethylamino group.[17,18] It can be seen from Figure 1 that the absorption maximum (λ_{abs}) is in the order **1b** > **1c** > **1a**. These trends are also observed in the other two series of compounds **2a**−**c** and **3a**−**c**. In general, the introduction of a strong electron donor may raise the energy level of the highest occupied molecular orbital (HOMO) of the D-π-A molecule. As a result, the energy gaps (E_g, Table 1) between the HOMO and the lowest unoccupied molecular orbital (LUMO) of series **1** compounds decrease (**1b** < **1c** < **1a**) with an increase of the electron-donating ability of the substituent in the D-π-A system.

Although compounds **1c** and **2c** have the same electron donor and electron acceptor, the different bridge unit (phenylvinyl for **1c** and thienylvinyl for **2c**) leads to a slight red-shift (about 8 nm) for the absorption maximum of **2c** compared with that of **1c** (Figure 2). It is well-known that the aromaticity of electron-rich five-membered thiophene is lower than that of six-membered benzene; therefore the thiophene unit can offer more effective conjugation than the benzene unit in the D-π-A system and thus the above-mentioned red-shift was observed.[19] Figure 2 also displays the absorption spectra of compounds **2c** and **3c** with the different electron acceptor. The absorption maximum

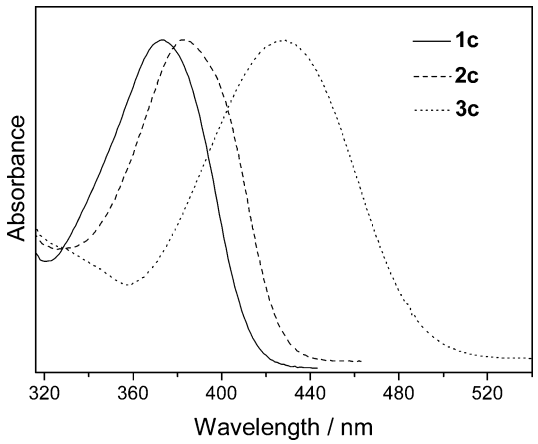

Figure 2. Absorption spectra of **1c** (solid, left), **2c** (dash, middle), and **3c** (dot, right) in 1:1 PhH/MeCN.

TABLE 2: Electrochemical[a] and ECL Characters of Series 1−3 in 1:1 PhH/MeCN

compound	$E_{pa}(1)$[b] (V)	E_{pc} (V)	E_{HOMO}[c] (eV)	E_{LUMO}[d] (eV)	λ_{ECL} (nm)	E_s[e] (eV)	$-\Delta H^\circ_{ann}$[f] (eV)
1a	0.33	−2.64	−4.94	−1.97	460	2.74	2.87
1b	0.31	−2.49	−4.92	−2.13	490	2.59	2.70
1c	0.85	−2.32	−5.33	−2.43	469	2.67	3.07
2a	0.53	−2.29	−5.13	−2.29	564	2.70	2.72
2c	0.77	−2.14	−5.29	−2.48	523	2.62	2.81
3a	0.64	−1.68	−5.23	−2.91	577	2.07	2.22
3b	0.43	−1.71	−5.01	−2.82	614	1.96	2.04
3c	0.91	−1.64	−5.47	−3.04	570	2.09	2.45

[a] vs SCE. [b] Only the first oxidation potentials are listed in Table 2. [c] $E_{HOMO}/eV = -4.74/eV - eE^{ox}_{onset}$.[21] [d] $E_{LUMO}/eV = E_g + E_{HOMO}$, the value of E_g can be seen from Table 1. [e] Calculated from the highest energy emission peak in fluorescence spectrum. [f] $-\Delta H^\circ_{ann}/eV = E_{pa}(1) - E_{pc}(1) - 0.1$ eV.[22]

of **3c** shows a large red-shift (>40 nm, Table 1) and a broad absorption band in comparison with **2c**. This can be ascribed to stronger π-electron conjugation system in **3c** containing an aldehyde group than **2c** containing a bromide group.

As shown in Table 1, the changes of fluorescence emission for each series have a similar trend. Comparing the Stokes shift ($\Delta\lambda_{st}$), both series **1** and **2** compounds show a very similar Stokes shift (around 90 nm); for series **3,** the shift is considerably larger (around 170 nm). This is attributed to the joint effect of the strong electron-withdrawing ability of the aldehyde group and the more effective conjugation in series **3** compounds resulting from the introduction of the thiophene unit. At the same time, the appearance of such a large Stokes shift suggests the occurrence of an intramolecular charge transfer (ICT) state from the electron donor to the electron acceptor.[14,20]

Electrochemistry. The redox potential values are crucial for ECL studies. The first oxidation potentials and the reduction potentials for all compounds are summarized in Table 2. Cyclic voltammograms of compounds **1a**, **2c**, and **3a** in a 1:1 PhH/MeCN solution with a sample concentration of 1×10^{-3} M and 0.05 M $TBAPF_6$ obtained at a platinum electrode using a nonaqueous Ag/Ag^+ reference electrode are shown in Figure 3. Due to the limitation of the potential window of the solvent, the cathodic reduction waves for series **1** and **2** compounds are not well-resolved; differential pulse voltammograms (DPV) display that they have clear cathodic reductions, which are shown as inset A and inset B of Figure 3. All compounds exhibit two successive one-electron oxidation waves, one reversible oxidation, and one irreversible oxidation. On the reduction side, one quasi-reversible or one irreversible one-electron reduction

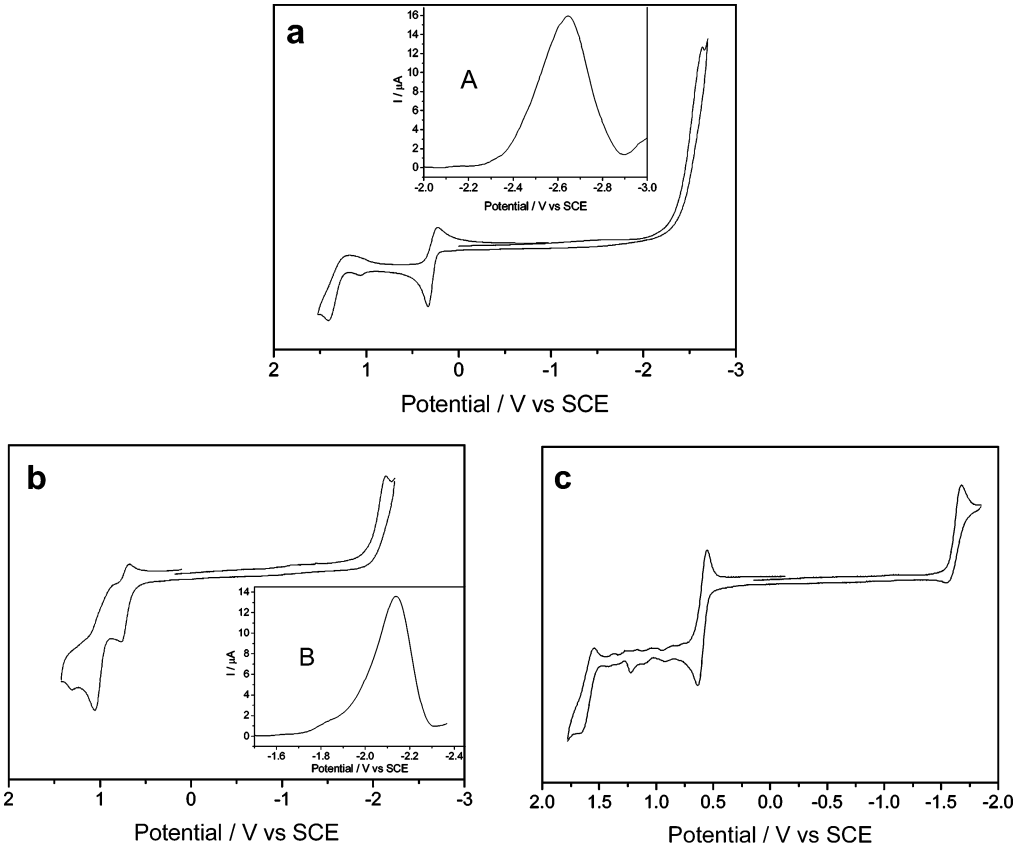

Figure 3. Cyclic voltammograms of **1a** (a), **2c** (b), and **3a** (c) with sample concentration of 1×10^{-3} M in 1:1 PhH/MeCN using a platinum working electrode and an Ag/Ag^+ reference electrode, scan rate 100 mV s^{-1}. Insets: DPVs of **1a** (A) and **2c** (B).

wave is observed for all compounds. The first oxidation peak potentials decrease and the HOMO energy levels increase with increasing electron-donating ability in every family. In addition, the experimental data indicate that the presence of the triphenylamine unit in the backbone decreases the HOMO and LUMO energy levels of compound **c** in all 3 series.

ECL and X-ray Crystal Structures. ECL spectra were recorded with a sample concentration of 1×10^{-3} M in the presence of 0.05 M $TBAPF_6$ as a supporting electrolyte in a 1:1 PhH/MeCN solution. ECL emission is produced by the annihilation reaction of a radical anion and a radical cation during repeated potential pulsing (pulse width = 0.5 s) between the compound's first oxidation potential and first reduction potential. The ECL data of series **1**−**3** are listed in Table 2. In order to clearly explain their ECL behavior, one compound will be taken from each series and discussed in detail.

The ECL maxima (λ_{ECL}) for series **1** compounds are in good agreement with their fluorescence maxima with deviations from 5 to 11 nm. Figure 4 shows the ECL and fluorescence spectra of compound **1b**. It can be observed that the emission curve and bandwidth of ECL are similar to those of fluorescence.

The X-ray crystal structure of compound **1b** (Figure 5) shows that the molecule has a nonplanar structure; the dihedral angle between the two benzene rings is determined to be 24.9°.[23] From the crystal-packing diagram, it can be seen that two donor moieties are stacked face to face with acceptor groups projecting away in opposing directions. The observed interplanar distance between the two parallel electron-donating groups of adjacent molecules is 4.09 Å. This long distance is beyond the range of a typical $\pi-\pi$ interaction,[10e,24] indicating very little interaction between the molecules of compound **1b** in solution. Furthermore, there is hardly any increase for the ECL intensity of

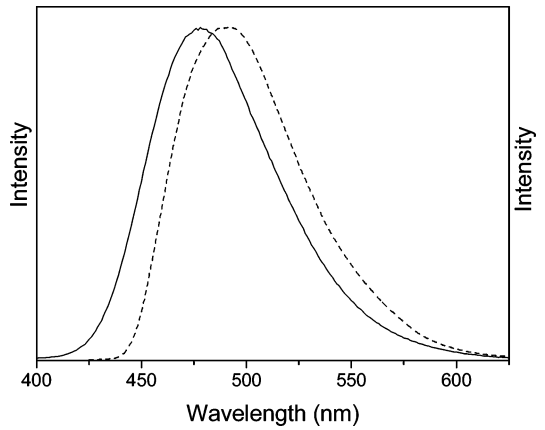

Figure 4. ECL (10^{-3} M, dash) and fluorescence (10^{-5} M, solid) spectra of **1b** in 1:1 PhH/MeCN.

compound **1b** with increasing the sample concentration from 1×10^{-5} M to 1×10^{-3} M (see Supporting Information, Figure S21). Thus, the ECL of series **1** compounds can be safely considered as the typical and simple monomer ECL emission resulting from the annihilation of radical cations and radical anions.

Unlike series **1** compounds, the ECL maxima of series **2** compounds shift significantly to the longer wavelength by 50−104 nm in comparison with their fluorescence maxima. Figure 6 shows the ECL and fluorescence spectra of compound **2a**. It can be observed that the ECL emission band is broader than the fluorescence emission band.

From the X-ray crystallographic analysis, we find that compound **2a** (Figure 7) also has a nonplanar structure. There is a slight twist between the benzene ring and the thiophene ring, and the dihedral angle is determined to be 4°.[25] From the

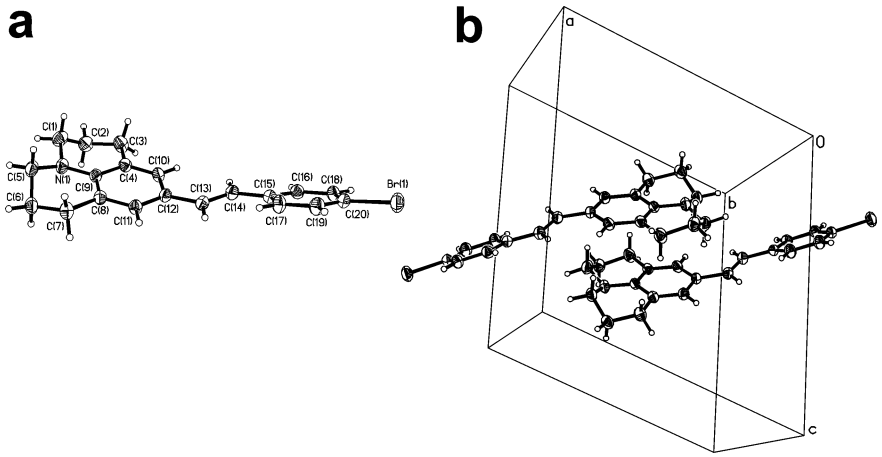

Figure 5. X-ray crystal structure (a) and crystal packing diagram (b) of compound **1b** with thermal ellipsoids set at 30% probability.

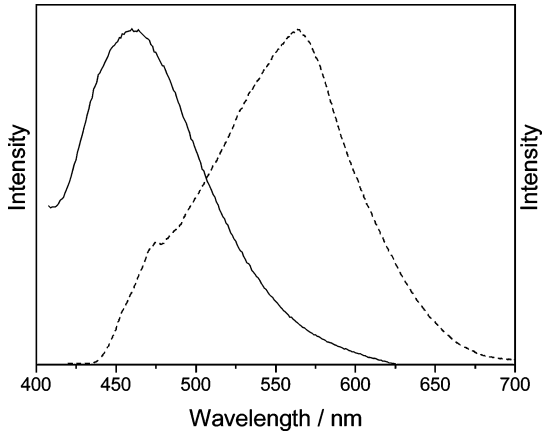

Figure 6. ECL (10^{-3} M, dash) and fluorescence (10^{-5} M, solid) spectra of **2a** in 1:1 PhH/MeCN.

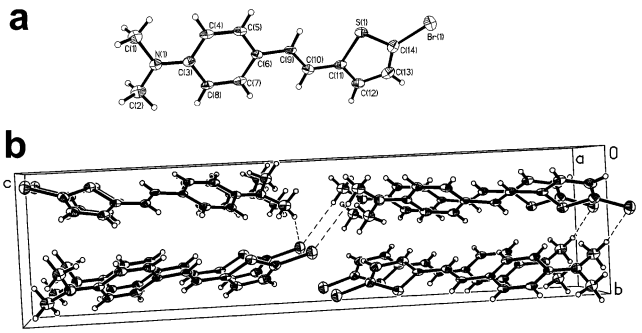

Figure 7. X-ray crystal structure (a) and crystal packing diagram (b) of compound **2a** with thermal ellipsoids set at 30% probability.

crystal packing diagram, it is observed that a Br atom from one molecule simultaneously interacts with two H atoms from another two molecules to form two weak intermolecular C−H···Br hydrogen bonds (the C···Br distances are 3.79 Å and 3.92 Å, respectively; ∠C−H···Br are 150.9° and 153.1°, respectively).[26] It is also found that the interplanar distance between the two parallel planes of adjacent molecules is 2.77 Å, which is within the range of a typical $\pi-\pi$ interaction.[10e,24] At higher concentration under ECL experimental conditions, the ECL-active species may reflect to a certain extent the real structure of π-stacking in the crystals as shown in Figure 7.[11b,27] Additionally, it has been observed that the ECL intensity of compound **2a** is obviously enhanced with the increase of the sample concentration from 1×10^{-5} to 1×10^{-3} M (see

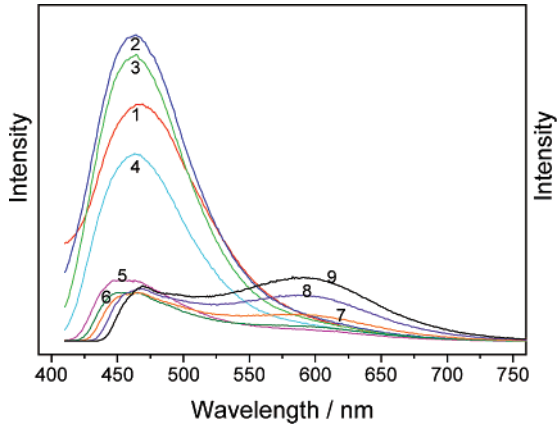

Figure 8. Fluorescence spectra of compound **2a** (1) 1×10^{-5} M (red), (2) 2.5×10^{-5} M (blue), (3) 5×10^{-5} M (green), (4) 1×10^{-4} M (cyan), (5) 2.5×10^{-4} M (magenta), (6) 5×10^{-4} M (olive), (7) 1×10^{-3} M (orange), (8) 2.5×10^{-3} M (violet), and (9) 7.5×10^{-3} M (black) in 1:1 PhH/MeCN.

Supporting Information, Figure S22). Thus, we can affirm the existence of an excimer formation during the ECL process.[27,28]

The excimer formation of compound **2a** can be further confirmed by its fluorescence properties at higher concentration. Figure 8 shows the fluorescence spectra of **2a** with different concentrations in 1:1 PhH/ MeCN solution excited at 390 nm. The monomer emission intensity at about 460 nm initially increases and then decreases with an increase in the sample concentration from 1×10^{-5} to 1×10^{-4} M. As shown in Figure 8, the fluorescence intensity is decreased dramatically at the concentration of 2.5×10^{-4} M. Subsequently, another new emission band appears around 591 nm when the concentration exceeds 2.5×10^{-4} M. As a result, we assign the new fluorescence emission band to be an excimer emission.

However, the absorption spectra of compound **2a** with different concentrations in 1:1 PhH/MeCN solution shows that the absorption maxima at 376 nm are invariable when the concentration is increased from 5×10^{-6} to 5×10^{-3} M (Figure 9). It can be considered that there is almost no aggregate formation at the ground state at higher concentration. Accordingly, we deduce that a charge-separated excited-state molecule can easily combine with a ground-state molecule to form an excimer during photoexcited fluorescence of series **2** compounds, which is similar to the excimer formed in ECL (Scheme 1).

In contrast to the red-shifts of series **1** and **2** compounds, the ECL maxima for series **3** compounds are blue-shifted by 19 to 24 nm in comparison with their fluorescence maxima. Figure

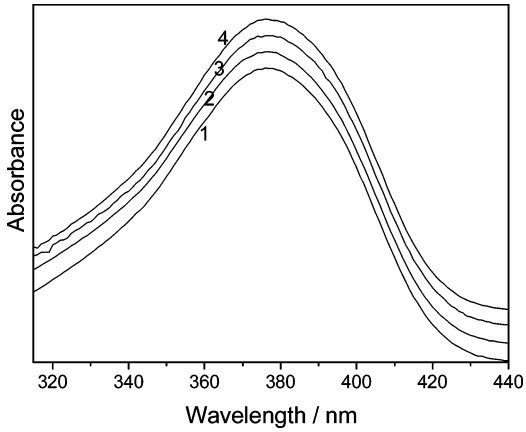

Figure 9. Absorption spectra (normalized) of compound **2a** (1) 5×10^{-6} M, (2) 1×10^{-5} M, (3) 1×10^{-3} M, and (4) 5×10^{-3} M in 1:1 PhH/MeCN.

SCHEME 1: Proposed Mechanisms for ECL Emission of Series 1− 3[a]

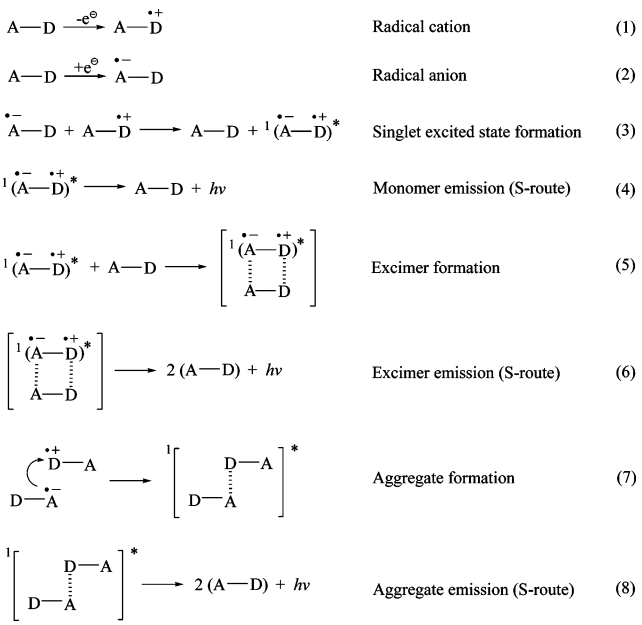

[a] **A** represents the acceptor moiety, and **D** represents the donor moiety in a molecule.

10 shows the ECL and fluorescence spectra of compound **3a**. It can be seen that the emission bandwidth of ECL is clearly narrower than that of fluorescence.

According to our previous study,[14a,29] the X-ray crystal structure of compound **3a** (Figure 11) is similar to that of **2a,** but with a few differences, it reveals an absolutely planar molecular structure, indicating an effective conjugation through the molecular axis. From the crystal-packing diagram, it indicates that two intermolecular C−H···O hydrogen bonds are formed (the C···O distances are 3.45 and 3.46 Å, respectively; ∠−C−H···O are 163.2° and 158.4°, respectively).[30] The interplanar distance between the two parallel planes of adjacent molecules is 2.63 Å, which shows strong interaction between the molecules of compound **3a**.[10e,24] At higher concentration under ECL experimental conditions, we expect that compound **3a** may exhibit a behavior similar to that of **2a**. However, it is quite the contrary. Unlike compound **2a**, there is almost no increase for the ECL intensity of compound **3a** when the sample concentration is enhanced (see Supporting Information, Figure S23).

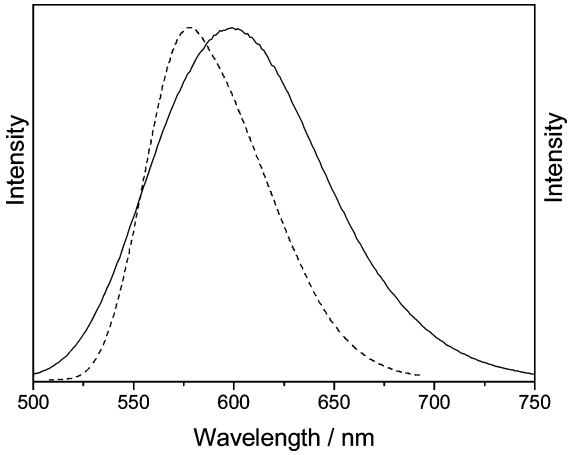

Figure 10. ECL (10^{-3} M, dash) and fluorescence (10^{-5} M, solid) spectra of **3a** in 1:1 PhH/MeCN.

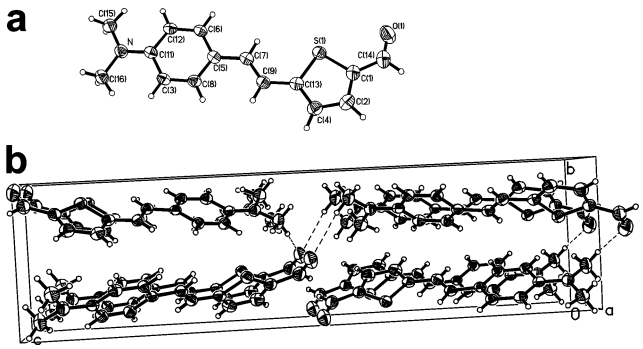

Figure 11. X-ray crystal structure (a) and crystal-packing diagram (b) of compound **3a** with thermal ellipsoids set at 30% probability.

By comparison, the fluorescence spectra of **3a** with different concentrations from 1×10^{-5} to 7.5×10^{-3} M are also obtained. We find that the fluorescence maxima are also invariable when the different solutions of **3a** are excited at 429 nm, despite the changes of emission intensity. Moreover, no new emission band is observed in the longer- or shorter-wavelength region (see Supporting Information, Figure S24).

However, the absorption maxima of compound **3a** are slightly shifted toward the longer wavelength from 426 to 434 nm when the concentration is increased from 1×10^{-5} to 5×10^{-3} M (see Supporting Information, Figure S25). This indicates that there are weak interactions between the molecules of compound **3a** at the ground state at higher concentration. Thus, there must be another ECL emission mechanism for series **3** compounds, which is different from that of series **1** and **2**. We propose that the ECL emission results from an aggregate formed via the interaction between a cation and an anion in the ground state under the ECL experimental conditions (Scheme 1).[11b]

To summarize these three series of compounds **1**−**3**, we found that the energy $-(\Delta H^\circ_{ann}$, listed in Table 2) provided by the ion-annihilation reaction, calculated from the peak potentials, is higher than the energy (E_s, listed in Table 2) required for direct production of the singlet state (Table 2):[22]

$$-\Delta H^\circ_{ann} > E_s$$

This means that the energy provided by the radical ions, for all compounds, is sufficient to produce a singlet excited state directly. As a result, the ECL emission of all compounds **1a**−**c**, **2a**−**c,** and **3a**−**c** can be observed via the singlet excited state.

The proposed mechanisms of ECL emission for series **1**, **2**, and **3** are represented in Scheme 1 (eqs 3 and 4 for series **1**, eqs 5 and 6 for series **2**, and eqs 7 and 8 for series **3**).

Conclusions

Three series of donor−acceptor π-conjugated (D-π-A) molecules **1**−**3** linked by a conjugated double bond have been synthesized. The absorption maxima of these compounds shift to longer wavelengths with the increasing electron-donating ability of the substituent in each series of compounds. Similar trends for the changes of their fluorescence emission are also observed. All compounds have good electrochemical stability, exhibiting two successive one-electron oxidation waves (one reversible oxidation and one irreversible oxidation). On the reduction side, one quasi-reversible or one irreversible one-electron reduction wave is observed. The electrogenerated radical ions are stable enough to produce an efficient ECL due to ion annihilation. As a result, series **1** shows a typical monomer ECL emission. The ECL emission for series **2** is proven to be an excimer emission. The blue-shifted ECL emission for series **3** can be attributed to an aggregate emission. X-ray crystal structures of compounds **1b**, **2a**, and **3a** provide further proof for the above-mentioned reaction mechanisms. All ECL emissions are observed without the addition of any co-reactant or additional compound. From the annihilation enthalpy changes of reaction, we propose that the ECLs for series **1**−**3** compounds are derived from the singlet excited state.

All series **1**−**3** compounds show good thermal, photochemical, and electrochemical stability as well as stable ECL emission. The interesting properties of these compounds may permit application in many fields such as photovoltaic devices, light-emitting devices, and bio-array analysis.

Acknowledgment. Financial support of this work from the following sources is gratefully acknowledged: the Programme of Introducing Talents of Discipline to Universities (Grant 20633020), China Natural Science Foundation (Grant 20128005), the Ministry of Science and Technology (MOST) (Grant 2001CCA02500), the Ministry of Education (MOE), the Swedish Energy Agency, the Swedish Research Council, and *K&A* Wallenberg Foundation. The authors thank Ping Li (DUT) for the analysis of X-ray data, Wenzhen Zhang (DUT) for very helpful discussions, and Dr. Alan Snedden (KTH) for the proofreading of this paper.

Supporting Information Available: Synthetic methodology for the preparation of intermediates **A**, **B**, and **C** and compounds **1a**−**c**, **2a**−**c**, and **3a**−**c**. NMR spectra for all compounds. Cyclic voltammograms and ECL spectra for **1a**, **1c**, **2c**, **3b**, and **3c**. This material is available free of charge via the Internet at http://pubs.acs.org.

References and Notes

(1) (a) Richter, M. M. *Chem. Rev.* **2004**, *104*, 3003. (b) Fähnrich, K. A.; Pravda, M.; Guilbault, G. G. *Talanta* **2001**, *54*, 531. (c) Knight, A. W. *Trends Anal. Chem.* **1999**, *18*, 47. (d) Knight, A. W.; Greenway, G. M. *Analyst* **1994**, *119*, 879. (e) Li, M.-J.; Chu, B. W.-K.; Yam, V. W.-W. *Chem. Eur. J.* **2006**, *12*, 3528.

(2) (a) Dennany, L.; Forster, R. J.; White, B.; Smyth, M.; Rusling, J. F. *J. Am. Chem. Soc.* **2004**, *126*, 8835. (b) Lin, J.-M.; Yamada, M. *Microchem. J.* **1998**, *58*, 105. (c) Chen, G. N.; Zhang, L.; Lin, R. E.; Yang, Z. C.; Duan, J. P.; Chen, H. Q.; Hibbert, D. B. *Talanta* **2000**, *50*, 1275. (d) Brune, S. N.; Bobbitt, D. R. *Anal. Chem.* **1992**, *64*, 166. (e) Kulmala, S.; Suomi, J. *Anal. Chim. Acta* **2003**, *500*, 21. (f) Yin, X.-B.; Qi, B.; Sun, X.; Yang, X.; Wang, E. *Anal. Chem.* **2005**, *77*, 3525.

(3) (a) Lai, R. Y.; Fabrizio, E. F.; Lu, L.; Jenekhe, S. A.; Bard, A. J. *J. Am. Chem. Soc.* **2001**, *123*, 9112. (b) Lai, R. Y.; Kong, X.; Jenekhe, S. A.; Bard, A. J. *J. Am. Chem. Soc.* **2003**, *125*, 12631.

(4) Dufford, R. T.; Nightingale, D.; Gaddum, L. W. *J. Am. Chem. Soc.* **1927**, *49*, 1858.

(5) (a) Cao, W.; Zhang, X.; Bard, A. J. *J. Electroanal. Chem.* **2004**, *566*, 409. (b) Lai, R. Y.; Fleming, J. F.; Merner, B. L.; Vermeij, R. J.; Bodwell, G. J.; Bard, A. J. *J. Phys. Chem. A* **2004**, *108*, 376. (c) Fabrizio, E. F.; Prieto, I.; Bard, A. J. *J. Am. Chem. Soc.* **2000**, *122*, 4996. (d) Lee, W. I.; Bae, Y.; Bard, A. J. *J. Am. Chem. Soc.* **2004**, *126*, 8358.

(6) (a) Miao, W.; Bard, A. J. *Anal. Chem.* **2004**, *76*, 7109. (b) White, H. S.; Bard, A. J. *J. Am. Chem. Soc.* **1982**, *104*, 6891. (c) Honda, K.; Yoshimura, M.; Rao, T. N.; Fujishima, A. *J. Phys. Chem. B* **2003**, *107*, 1653.

(7) (a) Choi, H. N.; Cho, S.-H.; Lee, W.-Y. *Anal. Chem.* **2003**, *75*, 4250. (b) Tokel, N. E.; Bard, A. J. *J. Am. Chem. Soc.* **1972**, *94*, 2862. (c) Ege, D.; Becker, W. G.; Bard, A. J. *Anal. Chem.* **1984**, *56*, 2413. (d) Yang, M.; Liu, C.; Hu, X.; He, P.; Fang, Y. *Anal. Chim. Acta* **2002**, *461*, 141.

(8) (a) Zu, Y.; Bard, A. J. *Anal. Chem.* **2000**, *72*, 3223. (b) Yin, X.-B.; Dong, S.; Wang, E. *Trends Anal. Chem.* **2004**, *23*, 432.

(9) (a) Debad, J. D.; Morris, J. C.; Magnus, P.; Bard, A. J. *J. Org. Chem.* **1997**, *62*, 530. (b) Lai, R. Y.; Bard, A. J. *J. Phys. Chem. B* **2003**, *107*, 5036. (c) Fungo, F.; Wong, K.-T.; Ku, S.-Y.; Hung, Y.-Y.; Bard, A. J. *J. Phys. Chem. B* **2005**, *109*, 3984. (d) Sartin, M. M.; Boydston, A. J.; Pagenkopf, B. L.; Bard, A. J. *J. Am. Chem. Soc.* **2006**, *128*, 10163.

(10) (a) Reshetnyak, O. V.; Kozlovs'ka, Z. E.; Koval'chuk, E. P.; Obushak, M. D.; Rak, J.; Blazejowski, J. *Electrochem. Commun.* **2001**, *3*, 1. (b) Okajima, T.; Ohsaka, T. *J. Electroanal. Chem.* **2002**, *534*, 181. (c) Chen, C.-Y.; Ho, J.-H.; Wang, S.-L.; Ho, T.-I. *Photochem. Photobiol. Sci.* **2003**, *2*, 1232. (d) Ho, T.-I.; Elangovan, A.; Hsu, H.-Y.; Yang, S.-W. *J. Phys. Chem. B* **2005**, *109*, 8626. (e) Elangovan, A.; Kao, K.-M.; Yang, S.-W.; Chen, Y.-L.; Ho, T.-I.; Su, Y. O. *J. Org. Chem.* **2005**, *70*, 4460. (f) Wong, K.-T.; Hung, T.-H.; Chao, T.-C.; Ho, T.-I. *Tetrahedron Lett.* **2005**, *46*, 855.

(11) (a) Elangovan, A.; Yang, S.-W.; Lin, J.-H.; Kao, K.-M.; Ho, T.-I. *Org. Biomol. Chem.* **2004**, *2*, 1597. (b) Elangovan, A.; Chiu, H.-H.; Yang, S.-W.; Ho, T.-I. *Org. Biomol. Chem.* **2004**, *2*, 3113.

(12) Lai, R. Y. Ph.D. Thesis, the University of Texas at Austin, 2003, Chapter 1.

(13) Velapoldi, R. A.; Tønnesen, H. H. *J. Fluoresc.* **2004**, *14*, 465.

(14) (a) Yang, X.; Jiang, X.; Zhao, C.; Chen, R.; Qin, P.; Sun, L. *Tetrahedron Lett.* **2006**, *47*, 4961. (b) Chen, R.; Zhao, G.; Yang, X.; Jiang, X.; Liu, J.; Tian, H.; Gao, Y.; Han, K.; Sun, M.; Sun, L. *Chem. Phys. Lett.*, submitted.

(15) Mehlhorn, A.; Schwenzer, B.; Schwetlick, K. *Tetrahedron* **1977**, *33*, 1489.

(16) McCord, P.; Bard, A. J. *J. Electroanal. Chem.* **1991**, *318*, 91.

(17) Yang, J.-S.; Chiou, S.-Y.; Liau, K.-L. *J. Am. Chem. Soc.* **2002**, *124*, 2518 and references therein.

(18) Thelakkat, M. *Macromol. Mater. Eng.* **2002**, *287*, 442.

(19) (a) Woo, H. Y.; Shim, H.-K.; Lee, K.-S. *Polym. J.* **2000**, *32*, 8. (b) Delgado, M. C. R.; Hernández, V.; Casado, J.; Navarrete, J. T. L.; Raimundo, J.-M.; Blanchard, P.; Roncali, J. *Chem. Eur. J.* **2003**, *9*, 3670. (c) Abbotto, A.; Bradamante, S.; Facchetti, A.; Pagani, G. A. *J. Org. Chem.* **1997**, *62*, 5755.

(20) Yang, J.-S.; Liau, K.-L.; Wang, C.-M.; Hwang, C.-Y. *J. Am. Chem. Soc.* **2004**, *126*, 12325.

(21) Ding, B.; Zhang, J.; Zhu, W.; Zheng, X.; Wu, Y.; Jiang, X.; Zhang, Z.; Xu, S. *Chin. J.Lumin.* **2003**, *24*, 606.

(22) Lee, S. K.; Zu, Y.; Herrmann, A.; Geerts, Y.; Müllen, K.; Bard, A. J. *J. Am. Chem. Soc.* **1999**, *121*, 3513.

(23) Crystal structure data for **1b**: $C_{20}H_{20}BrN$, $M_r = 354.28$, monoclinic, space group: $P2(1)/n$, $a = 12.0445(19)$, $b = 11.0193(17)$, $c = 12.895(2)$ Å, $\alpha = \gamma = 90°$, $\beta = 109.308°(2)$, $V = 1615.2(4)$ Å^3, $T = 273(2)$ K, $Z = 4$, $F(000) = 728$, $D_c = 1.457$ g cm^{-3}, $R = 0.0353$, $R_w = 0.0788$, GOF = 0.879. CCDC-606888 contains the supplementary crystallographic data for this article. These data can be obtained free of charge from The Director, CCDC, 12 Union Road, Cambridge, CB21EZ, UK (Fax: +44-1233-336-033; e-mail: deposit@ccdc.cam.ac.uk or http://www.ccdc.cam.ac.uk).

(24) (a) Steed, J. W.; Atwood, J. L. *Supramolecular Chemistry*; Chichester: John Wiley & Son, 2000; p 26. (b) Coates, G. W.; Dunn, A. R.; Henling, L. M.; Ziller, J. W.; Lobkovsky, E. B.; Grubbs, R. H. *J. Am. Chem. Soc.* **1998**, *120*, 3641.

(25) Crystal structure data for **2a**: $C_{14}H_{14}BrNS$, $M_r = 308.23$, orthorhombic, space group: $P2(1)2(1)2(1)$, $a = 5.9341(8)$, $b = 7.5579(10)$, $c = 29.632(4)$ Å, $\alpha = \beta = \gamma = 90°$, $V = 1329.0(3)$ Å^3, $T = 273(2)$ K, $Z = 4$, $F(000) = 624$, $D_c = 1.541$ g cm^{-3}, $R = 0.0674$, $R_w = 0.1607$, GOF = 1.045. CCDC-616425 contains the supplementary crystallographic data for this article. These data can be obtained free of charge from The Director,

CCDC, 12 Union Road, Cambridge, CB21EZ, UK (Fax: +44-1233-336-033; e-mail: deposit@ccdc.cam.ac.uk or http://www.ccdc.cam.ac.uk).

(26) (a) Golovanov, D. G.; Lyssenko, K. A.; Antipin, M. Y.; Vygodskii, Y. S.; Lozinskaya, E. I.; Shaplov, A. S. *Cryst. Growth Des.* **2005**, *5*, 337. (b) Bowmaker, G. A.; Boyd, P. D. W.; Rickard, C. E. F.; Scudder, M. L.; Dance, I. G. *Inorg. Chem.* **1999**, *38*, 5476.

(27) Elangovan, A.; Lin, J.-H.; Yang, S.-W.; Hsu, H.-Y.; Ho, T.-I. *J. Org. Chem.* **2004**, *69*, 8086.

(28) (a) Prieto, I.; Teetsov, J.; Fox, M. A.; Bout, D. A. V.; Bard, A. J. *J. Phys. Chem. A* **2001**, *105*, 520. (b) Choi, J.-P.; Wong, K.-T.; Chen, Y.-M.; Yu, J.-K.; Chou, P.-T.; Bard, A. J. *J. Phys. Chem. B* **2003**, *107*, 14407.

(29) Please refer to the new deposited data of compound **3a**: CCDC-635847.

(30) (a) Desiraju, G. R. *Acc. Chem. Res.* **1996**, *29*, 441. (b) Fourmigué, M.; Batail, P. *Chem. Rev.* **2004**, *104*, 5379.